ACS Biomaterials SCIENCE & ENGINEERING

pubs.acs.org/journal/abseba Article

Detection of Kallikrein-Related Peptidase 4 with a Label-free Electrochemical Impedance Biosensor Based on a Zinc(II) Phthalocyanine Tetracarboxylic Acid-Functionalized Disposable Indium Tin Oxide Electrode

Elif Burcu Aydın, Muhammet Aydın, Abdulcelil Yuzer, Mine Ince, Kasim Ocakoğlu, and Mustafa Kemal Sezgintürk*

Cite This: *ACS Biomater. Sci. Eng.* 2021, 7, 1192−1201 Read Online

ACCESS | Metrics & More | Article Recommendations | Supporting Information

ABSTRACT: A new impedimetric biosensing system based on kallikrein-related peptidase 4 (KLK 4) antigen-specific antibodies and a zinc(II) phthalocyanine tetracarboxylic acid (Zn-PcTCa) matrix material was developed for the first time in this study. First, a Zn-PcTCa-coated indium tin oxide surface was used as an interface matrix material for the immobilization of anti-KLK 4 antibodies, and they bound to the platform via amide bonds. In the presence of KLK 4 antigens, the anti-KLK 4 antibodies specifically captured these antigens and caused changes in the electrochemical properties of the system. Randles equivalent circuit was utilized to evaluate the impedimetric signal, which was measured with the help of an electrochemical impedance spectroscopy method. After the specific interaction, the electron transfer resistance (R_{ct}) was remarkably increased and displayed a linear relationship with the level of the KLK 4 antigen in the range of 0.02−15 pg/mL, with a a detection limit of 6.8 fg/mL. The designed biosensor was able to detect a KLK 4 antigen with good sensitivity, excellent specificity, and high stability. In addition, because of having a low-cost and robust procedure for fabrication, it could be repeatedly used in several areas including clinical diagnosis.

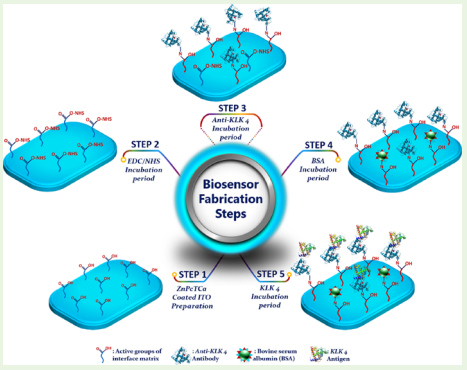

KEYWORDS: *tetracarboxylic acid, kallikrein-related peptidase 4, metallophthalocyanines, electrochemical impedance spectroscopy, biosensor*

Downloaded via BUTLER UNIV on May 16, 2021 at 13:11:33 (UTC).
See https://pubs.acs.org/sharingguidelines for options on how to legitimately share published articles.

1. INTRODUCTION

Prostate cancer is one of the major health threats worldwide, and this disease is the third most diagnosed cancer type in men who are older than 50 years.[1] According to estimates from the World Health Organization in 2018, 1.3 million new prostate cases have been diagnosed, with 1.7 million incidences and 0.5 million annual mortality rates by 2030. The important approach to reduce the mortality risk is early and accurate diagnosis of prostate cancer. For the prognosis of prostate cancer, imaging methods are preferred because they provide precise disease monitoring including their anatomy and functionality. Apart from imaging techniques, ultrasonography, computed tomography, digital rectal examination, magnetic resonance imaging, and tumor marker immunoassay have been utilized.[2] Though these techniques are robust and successful for prostate cancer diagnosis, they have low sensitivity, low specificity, and require a lot of time for procedure application. Therefore, new, sensitive, and low-cost techniques are required.[3]

Kallikreins are a subgroup of the serine protease enzyme family. The human tissue kallikrein gene family codes for 15 highly conserved serine proteases with either trypsin or chymotrypsin-like substrate specificity. Kallikreins are expressed in several tissues such as the tissues producing steroid hormone, hormone-dependent tissues including prostate, breast, ovary, and testis.[4,5] Until now, a prostate-specific antigen (PSA) is the well-known tumor biomarker related to the existence and progression of prostate cancer. Upon the usage of the PSA as a prostate cancer biomarker, some problems including false positive results in patients with benign prostatic hyperplasia and false negative results in patients with other residual disease have been monitored. Because of these causes, new prostate cancer markers are required.[5] KLK 4 is a candidate tumor biomarker for prostate cancer. KLK 4 is

Received: November 12, 2020
Accepted: February 9, 2021
Published: February 15, 2021

© 2021 American Chemical Society

https://dx.doi.org/10.1021/acsbiomaterials.0c01602
ACS Biomater. Sci. Eng. 2021, 7, 1192−1201

Table 1. Techniques of KLK 4 Analysis (a); the Results of Human Serum Samples with the Proposed Biosensor (B)

(A) technique	linear range (pg/mL)	limit of detection (pg/mL)	reference
Zn-PCTCa-modified ITO electrode	0.02−15	0.0068	this study
SucS-PThi-modified ITO electrode	0.04−30	0.0122	39
ELISA-colorimetric	31.25−2000	18.75	Elabscience
ELISA-colorimetric	2000−32,000	100	MyBiosource
ELISA-colorimetric	156−10,000	390	Cusabio
ELISA-colorimetric	312−20,000	113	Cloud-Clone Corp.
ELISA-colorimetric	2460−600,000	2000	Thermofisher

(B) sample	found by biosensor (pg/mL)	added KLK 4 antigen (pg/mL)	*SD and *CV (%)	total found by the biosensor	*SD and *CV (%)	recovery (%)	relative difference (%)
1	2.16	1	0.01, 0.37	3.25	0.04, 1.13	102.88	2.88
1	2.17	1		3.19		100.88	0.88
2	3.82	1	0.041, 0.21	4.93	0.02, 0.41	102.30	2.30
2	3.83	1		4.96		102.65	2.65
3	3.06	1	0.08, 2.66	4.08	0.01, 0.30	100.55	0.55
3	3.07	1		4.10		98.14	−1.86
4	3.17	1	0.06, 1.89	4.13	0.03, 0.83	99.30	−0.70
4	3.15	1		4.17		98.44	−1.56
5	2.99	1	0.02, 0.74	4.03	0.01, 0.35	100.99	0.99
5	3.02	1		4.01		99.70	−0.30

produced in basal and secretory cells of the prostate gland and is overexpressed in malignant prostate tumors. Different researches have illustrated that KLK 4 has proteolytic activities, which are strongly associated to the development and progression of cancer.[6] The KLK 4 level in human serum of prostate cancer (PCa) patients is measured as ≤0.04 ng/mL[4]. For the measurement of the KLK 4 antigen in human serum samples, enzyme-linked immunosorbent assay (ELISA) has been used, and the essential principle of this system is based on a sandwich assay that is composed of one capture antibody and one detection antibody.[4] The usage of the ELISA technique has some disadvantages such as requirement of a specific laboratory, expensive device and experienced personnel, and long and extensive pre-treatment stages. Compared to the ELISA technique, electrochemical techniques have gained considerable attention because of their outstanding sensitivity, excellent stability and miniaturization, cost-effectiveness, short analysis durations, and environment-friendly feature.[7] Until now, no biosensors have been fabricated for the determination of the KLK 4 antigen. Only an impedimetric biosensor based on conducting succinimide group-substituted polythiophene polymer (SucS-PThi)-coated indium tin oxide (ITO) was developed in our previous study, and with this research, an ultrasensitive and selective immunosensor was developed. The performance of the proposed immunosensor was compared with ELISA kits, as displayed in Table 1A. As seen Table 1A, our biosensor had a lower detection limit than other studies. Compared to the ELISA kits, the developed immunosensor did not require excessive chemical use and it had a low-cost, simple, and short assay procedure, and a fast response. Furthermore, it could be reused for many measurements.

Metallophthalocyanines are planar 18-electron conjugated materials, and they are a well-known type of N4-macrocyclic metal compounds. Because of their suitable chemical and thermal stability, design flexibility, and excellent electrochemical features, they have been widely used as biosensing matrices for determination of different biological analytes containing dopamine, epinephrine, glucose, and choline.[8] In addition, they are considered as nanoenzymes due to their excellent peroxidase activity. They can serve as an electron mediator and be utilized as a horseradish peroxidase enzyme during the quantification of H_2O_2. This property makes them a low-cost alternative to replace enzymes.[9] Different metallophthalocyanines with different cores, such as Co^{II}, Zn^{II}, Cu^{II}, and Ni^{II}, have been developed due to the ease of synthesis and production with high yield.[10] The different metal centers of metallophthalocyanines have a potential to affect the catalytic activity, sensitivity, and selectivity of the whole Pc systems.For example, Li and co-workers' fabricated phthalocyanines-metal-graphene oxide hybrid materials for ammonia sensing.[11] They reported that different central metals of metallophthalocyanine played an important role showing a gradual decrease in the sensing activity of ammonia in the following order: Co > Cu > Ni > Fe ≫ GO.

Göktuğ et al. developed an amperometric biosensor modified with a zinc(II) phthalocyanine-bearing EDOT group for glucose sensing. This zinc(II) phthalocyanine-substituted PEDOT polymer was utilized for glucose oxidase immobilization and offered a new functional polymeric system. This biosensor illustrated a wide linear detection range (0.1−1.5 mM) and a low detection limit (0.049 mM).[12] In another study, a graphene oxide−cobalt(II) phthalocyanine (CoPc)-modified paper electrode was developed for H_2O_2 and glucose determinations. For glucose sensing, the glucose oxidase enzyme was attached onto the paper electrode. CoPc suspended nanoparticles served as a nanoenzyme mimicking peroxidase activity. The linear detection ranges of this system were found as 12 μM−49 mM for H_2O_2 and 0.1−1 mM for glucose.[9]

A label-free electrochemical immunosensor as a unique quantitative technique for the determination of several target analytes has been in the spotlight over the years, because of its excellent sensitivity, promising selectivity, easy-to-use property, fast detection, and low-cost instrumentation.[13] Its successful applications in the determination of several disease biomarkers containing alpha-fetoprotein,[14,15] a prostate-specific antigen,[16,17] interleukin 6,[18,19] interleukin 1β,[20,21] p53,[20] a neuron-specific antigen,[22] and interleukin 1α[23] have been reported so far. Electrochemical impedance spectroscopy (EIS) is a label-free, successful, nondestructive, and illuminat-

https://dx.doi.org/10.1021/acsbiomaterials.0c01602
ACS Biomater. Sci. Eng. 2021, 7, 1192−1201

Scheme 1. Schematic Representment of the Proposed Impedance Immunosensor Based on Zinc(II) Phthalocyanine for Sensitive Detection of KLK4

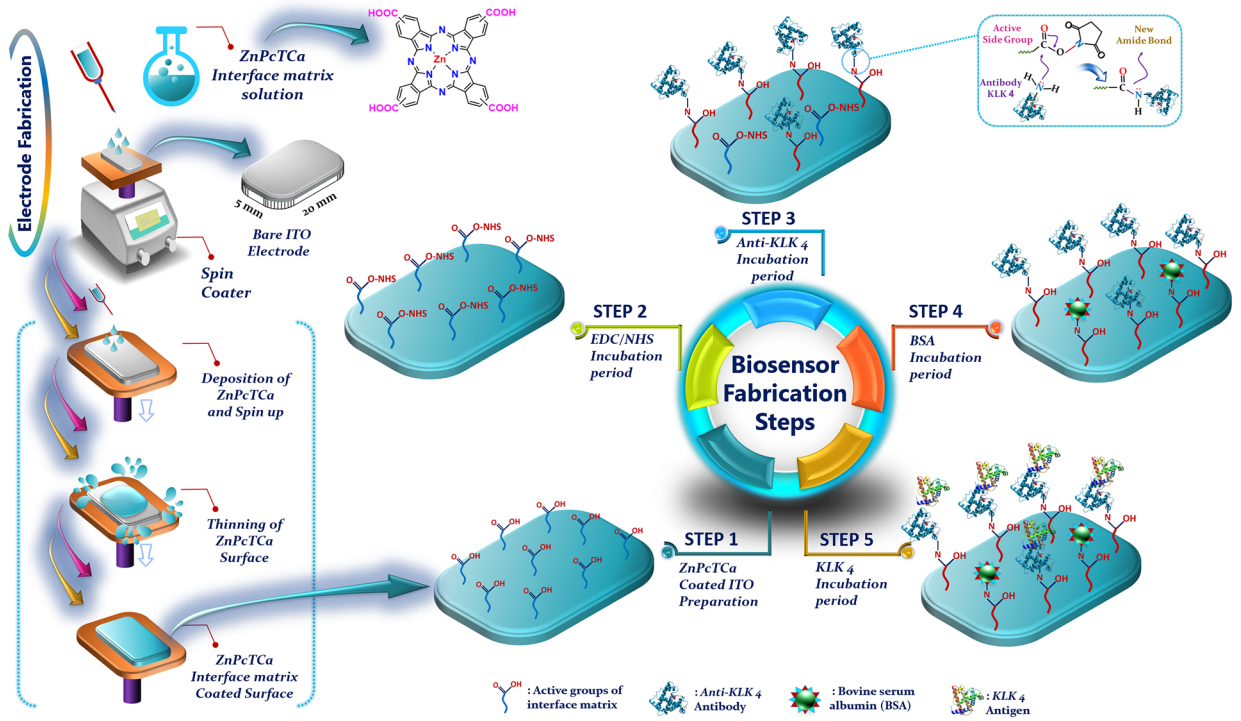

ing technique, and it is usually utilized to determine antigen−antibody interaction on the working electrode platforms by measurement of their capacitance and interfacial charge-transfer resistance.[23]

A critical step in immunosensor design is the immobilization of an antibody on the solid support.[25−27] Covalent attachment provides an irreversible binding of the biomolecule and protects its activity. A functionalized electrode can be convenient for a covalent binding of biological molecules for development of a biosensing tool.[28] In this study, for the first time, a novel approach using a zinc(II)-phthalocyanine tetracarboxylic acid (Zn-PcTCa)-modified ITO surface was developed for biosensing of KLK 4, a prostate cancer marker. So far, there are different studies on biosensor applications of phthalocyanine-based composites. Phthalocyanines have been utilized as a part of an active layer in biosensor fabrication. In order to construct the immobilization platform, it was prepared via incorporation of phthalocyanines with conductive polymers, carbon nanotubes, or graphene oxide. In these studies, the terminal groups of conductive polymers, carbon nanotubes, or graphene oxide were used as attachment points for immobilization of biomolecules. The use of Zn-PcTCa-containing carboxyl groups as an immobilization matrix provided low-cost biosensor fabrication, and the fabrication procedure of the biosensor was fast since no other materials, such as graphene oxide, carbon nanotubes, or conductive polymer, were synthesized. Before the fabrication of the biosensor, first, Zn-PcTCa was synthesized and used as a matrix material part in the biosensor construction. Zn-PcTCa was an efficient support due to its carboxyl groups, and the covalent linking of antibodies was achieved on the carboxyl-terminated ITO electrode surface. To link anti-KLK 4 antibodies, carboxyl groups of Zn-PcTCa were activated with the mixture of 1-ethyl-3-(3-dimethylaminopropyl)-carbodiimide (EDC) and *N*-hydroxysuccinimide (NHS) solution. The surface of Zn-PcTCa-modified ITO electrodes and the immobilization of the antibody onto modified ITO electrodes were electrochemically monitored with EIS and cyclic voltammetry (CV) techniques. Moreover, the morphological investigations for the different biosensor surfaces were made by scanning electron microscopy (SEM), SEM−EDX, and atomic force microscopy (AFM). Owing to the large surface-to-volume ratio and good biocompatibility of Zn-PcTCa, the suggested biosensor had good selectivity and sensitivity for KLK 4 detection. In addition, the suggested biosensing system could meet the requirements for direct determination of the KLK 4 antigen in human serum samples, illustrating a promising tool for clinical monitoring. Moreover, by using this approach, a simple, easily prepared, inexpensive, and disposable immunosensor was developed for KLK 4 determination.

2. EXPERIMENTAL SECTION

2.1. Materials and Reagents. Potassium ferricyanide(III), potassium ferrocyanide(II) trihydrate, dipotassium hydrogen phosphate, potassium dihydrogen phosphate, potassium chloride, EDC, and NHS were obtained from Sigma−Aldrich, U.S.A. Anti-KLK 4 antibody (rabbit), KLK 4 antigen (human), interleukin 6 (IL 6), prostate specific membrane antigen (PSMA), interleukin 1α (IL 1α), and bovine serum albumin (BSA) proteins were from Sigma−Aldrich, U.S.A. Phosphate buffered saline (PBS; pH 7.4, 50 mM) was used for anti-KLK 4, KLK 4 proteins, and other interference antigen solution preparation.

2.2. Apparatus. Electrochemical analyses were performed by using the Gamry Reference 1000 electrochemical workstation (U.S.A.) with a conventional three-electrode system that contained an ITO-coated polyethylene terephthalate (PET) working electrode, a platinum wire counter electrode, and an Ag/AgCl reference electrode. The electrode modification stages were monitored with EIS and CV measurements. CV analysis was carried out in a potential range from 0

https://dx.doi.org/10.1021/acsbiomaterials.0c01602
ACS Biomater. Sci. Eng. 2021, 7, 1192−1201

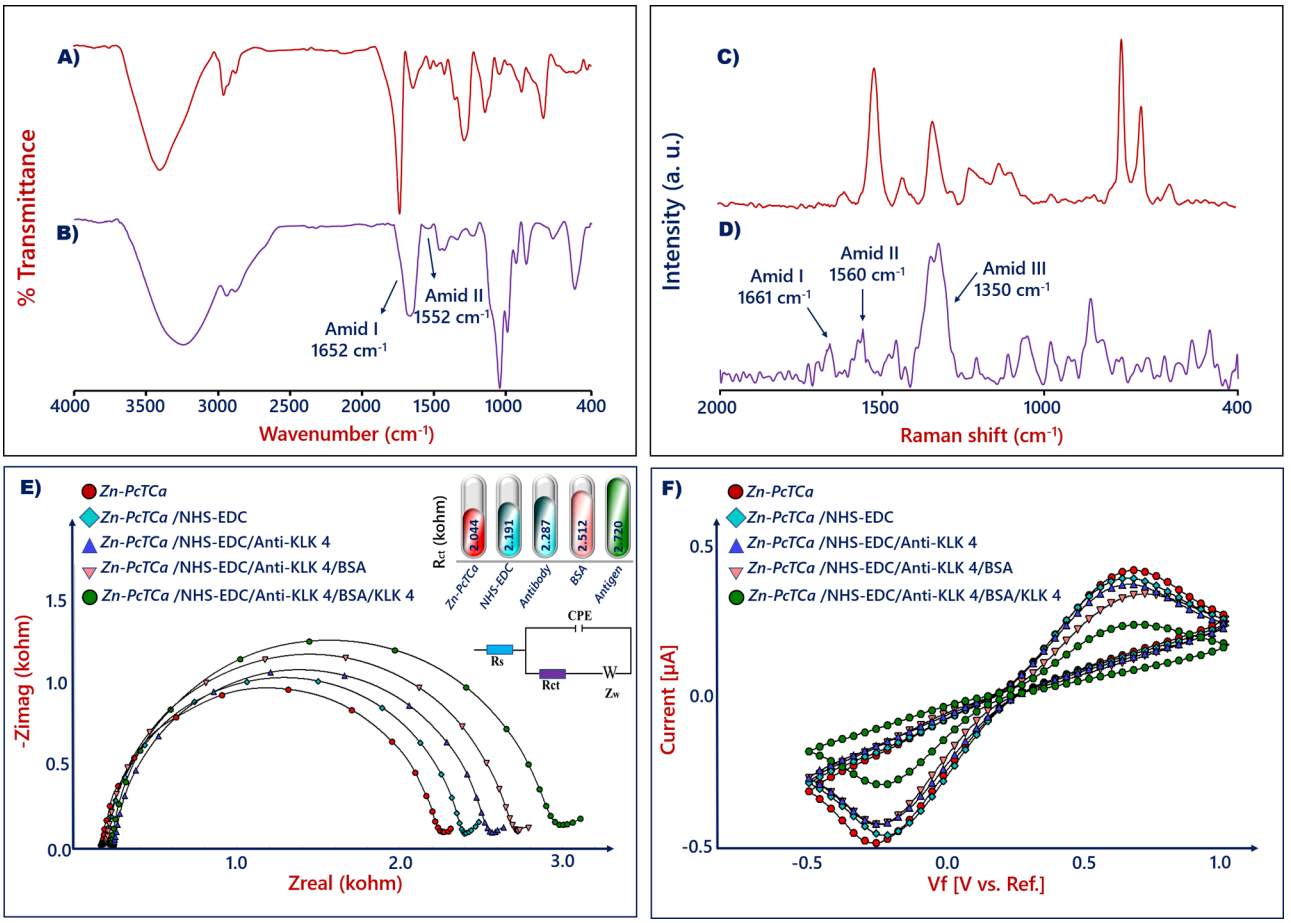

Figure 1. FTIR (A, B) and Raman (C, D) spectra before and after anti-KLK4 attachment. The Nyquist plots (E), CVs (F), and equivalent circuit (E, inset) after the modification procedure; electrochemical measurements were carried out in 5 mM $Fe(CN)_6^{3-/4-}$ and 1 M KCl.

to −0.5 V at a scan rate of 100 mV/s. The initial and final frequencies used in EIS analysis were 50,000 and 0.05 Hz, respectively. Infrared spectroscopy analysis was performed with a Bruker spectrometer in the wavenumber range of 400−4000 cm^{-1}. The Raman spectra were taken on a ThermoFisher Scientific DXR Raman spectrometer with a 780 nm laser in the range of 2000−400 cm^{-1}. The electrode surface morphology was investigated by SEM, SEM−EDX (FEI-Quanta FEG 250, U.S.A.), and AFM (NanoMagnetics, Turkey). The MALDI-TOFMS spectrum was determined on a Bruker Microflex LT. UV−vis spectrum was taken with a PerkinElmer spectrophotometer. X-ray photoelectron spectroscopy (XPS) measurements were performed with an XPS system (Specs-FlexPS model, Germany).

2.3. Synthesis of Zn-PcTCa. Zn-PcTCa, peripherally functionalized with carboxyl groups, was prepared according to the literature procedure using trimellitic anhydride, urea, and ammonium molybdate as a catalyst in the presence of anhydrous $ZnCl_2$ salt.[28] The synthesis of Zn-PcTCa was carried out in two steps starting from symmetrical tetra-formamido ZnPc, which was subjected to a hydrolysis reaction to yield the tetracarboxylic acid Zn-PcTCa. Thus, Zn-PcTCa was obtained as a green solid in 70% yield. The related chemical characterizations are given in the Supporting Information (Figures S1 and S2). UV−vis (DMSO) λmax (log ε): 683 (5.26), 619 (5.81), 349 (5.58). IR (ATR) ν (cm^{-1}): 2904, 1676, 1515, 1335, 1226, 1080, 920, 828, 733, 655, 468. MS (MALDI, dithranol): m/z: 752.979 [M^+].

Otherwise, X-ray photoelectron spectroscopy (XPS) measurements were performed on a Specs-Flex mode instrument. The samples (Zn-PcTCa) were analyzed by XPS spectroscopy to confirm the formation of the Zn-PcTCa. Integration of the Zn-PcTca was confirmed in our study by XPS measurements, in which C 1s, N 1s, O 1s, Zn $2p_{1/2}$, and Zn $2p_{3/2}$ contributions from the Zn-PcTca structures were identified. The broad-scan XPS analysis of Zn-PcTCa is shown in Figure S3. The XPS spectra reveal the presence of carbon, oxygen, nitrogen, and zinc in Zn-PcTCa, and the signals corresponding to C 1s, O 1s, N 1s, Zn $2p_{1/2}$, and Zn $2p_{3/2}$ were determined at 284.1, 530.3, 400,5, 1403, and 1020 eV, respectively (Figure S3). Oxygen, carbon, nitrogen, and zinc are the main components for ZnPc-TCa.

2.4. Fabrication of a Zn-PcTCa-Modified KLK 4 Biosensor. The biosensor was fabricated as demonstrated in Scheme 1. First, ITO-PET was sequentially ultrasonicated in acetone, soap solution, and ultrapure water for 10 min. Then, the pretreated ITO was dried under argon gas and placed on the spin-coater. The Zn-PcTCa dissolved in dimethyl sulfoxide (DMSO)/tetrahydrofuran (THF)/Acetone solution was dropped on the working electrode surface, and this surface was coated with Zn-PcTCa by using a spin-coater (1000 rpm, 60 s). The Zn-PcTCa-coated electrodes were dried at room temperature (step 1). Subsequently, the ITO/Zn-PcTCa electrode was immersed into NHS/EDC solution (0.1 mM:0.4 mM) for 1 h to activate the ITO electrode surface before incubation of the anti-KLK 4 solution (step 2). Then, the Zn-PcTCa-coated active ITO electrode was immersed in anti-KLK 4 solution to form a biorecognition layer (step 3). Active carboxyl groups bound to amino groups of anti-KLK 4 antibodies via an amide bond, and the ITO/Zn-PcTCa/anti-KLK 4 electrode was constructed. The unbound anti-KLK 4 antibodies were removed by washing with ultrapure water and dried under argon gas. The free active carboxyl groups were blocked by BSA (step 4). Subsequently, the prepared electrodes were incubated in different levels of the KLK 4 antigen (step 5). To eliminate any unbounded KLK 4 antigen present on the ITO electrodes, they were washed with ultrapure water.

https://dx.doi.org/10.1021/acsbiomaterials.0c01602
ACS Biomater. Sci. Eng. 2021, 7, 1192−1201

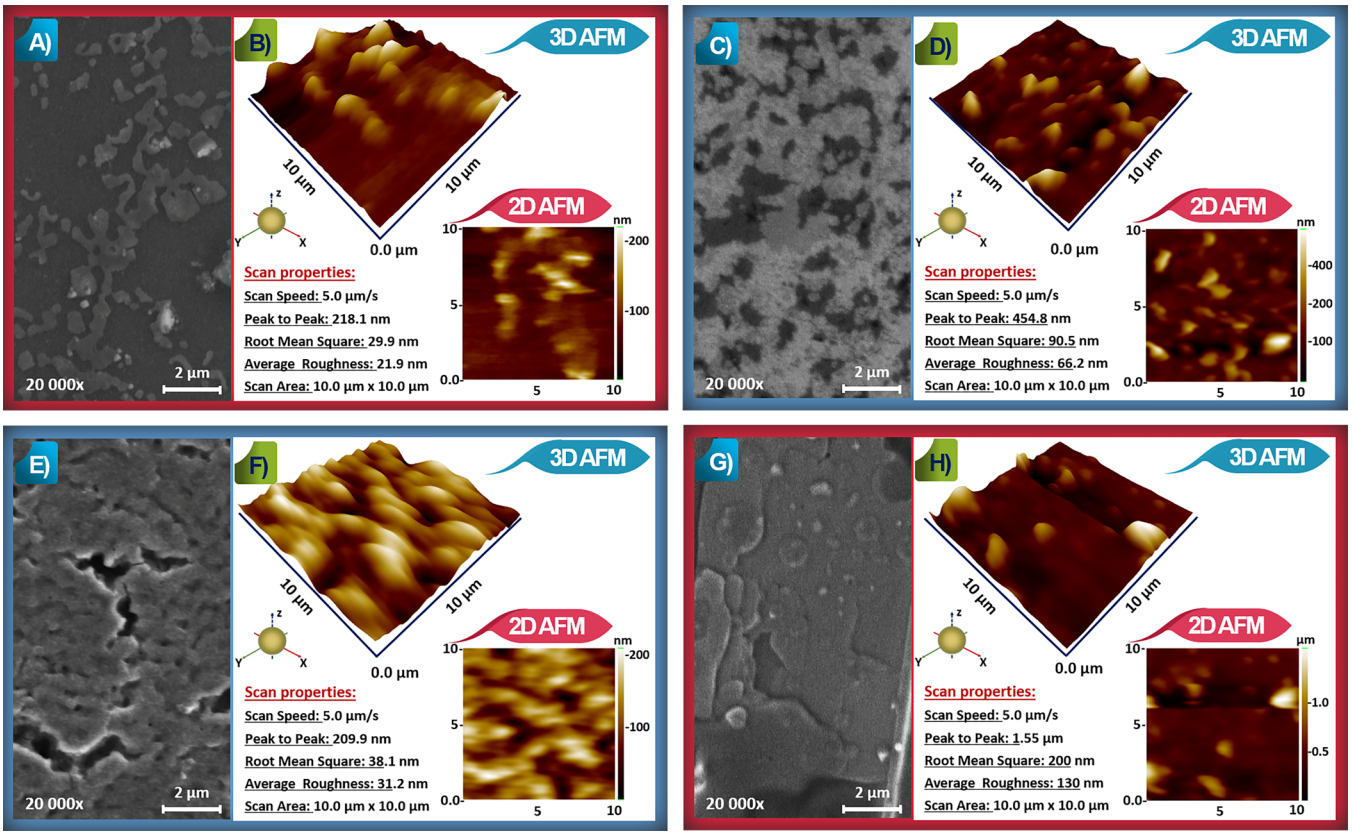

Figure 2. SEM and AFM appearances of the Zn-PcTCa-coated ITO substrate (A, B), and an anti-KLK 4 antibody covalently immobilized onto the electrode surface (C, D), BSA (E, F), and KLK 4 antigen (G, H).

3. RESULTS AND DISCUSSION

The discussion of the results was divided into five sections. First, the chemical characterizations of the Zn-PcTCa-modified electrode and anti-KLK 4 antibody attached to the ITO surface were explained. Second, the electrochemical characterizations of the electrode modification stages were discussed. Third, the morphological characterizations of fabricated electrode surfaces were investigated. Fourth, the optimization of conditions, which were necessary for biosensor fabrication, were discussed. Also the last one, the analytical characterization of the immunosensor was presented.

3.1. Chemical Characterization of the Zn-PcTCa-Coated and Anti-KLK 4 Antibody Attached ITO Surface. To identify the chemical structure of the Zn-PcTCa-coated (red) and anti-KLK 4-modified (purple) ITO surface, FTIR and Raman measurements were carried out, as displayed in Figure 1.

As observed in Figure 1A, for Zn-PcTCa-modified ITO, Zn-PcTCa had carboxyl groups and had the characteristic C═O bands at 1722 cm^{-1} and O−H bands at ∼3400 cm^{-1} in the spectrum.[30,31] The peak at around 1276 cm^{-1} were attributed to the C—N═ stretching vibration of Zn-PcTCa.[32] The phthalocyanine skeletal vibrations peaks showed at around 1140, 1090, 1043, 900, and 730 cm^{-1}.[29] In the FTIR spectra of Figure 1B, the new absorption peaks at 1652 (amid 1) and 1552 cm^{-1} (amid 2) illustrated the covalent linking between active carboxyl ends of the interface material and amino group of anti-KLK 4. Apart from the FTIR technique, Raman spectroscopy was utilized for chemical characterization. The Raman spectra of the Zn-PcTCa-coated electrode (red) and anti-KLK 4 immobilized electrode (purple) are shown in Figure 1C,D, respectively. The Raman spectra in Figure 1C displayed the similar peaks found in FTIR spectra after Zn-PcTCa coating. Amide I, amide II, and amide III bonds of proteins are generally seen between 1650−1680, 1480−1570, and 1235−1300 cm^{-1}, respectively.[33] The bands at 1661, 1560, and 1350 cm^{-1} were amide bonds formed on the ITO surface.

Furthermore, the surface modification with Zn-PcTCa was monitored by utilizing SEM−EDX measurement. As seen in Figure S4A, an SEM−EDX image of bare ITO had oxygen (O), indium (In), and tin (Sn) elements. After the spin-coating process, the SEM−EDX image of the coated electrode (Figure S4B) illustrated carbon (C), oxygen (O), nitrogen (N), and zinc (Zn) elements. The ratios of N and Z elements on different areas of the ITO electrodes were similar, and these close ratios of N and Zn elements displayed that the surface was covered homogenously with Zn-PcTCa.

3.2. Electrochemical Characterization of the KLK 4 Biosensor Construction Steps. Each step of the construction process of the biosensor was electrochemically analyzed using EIS and CV, as displayed in Figure 1E,F. EIS provides more efficient information about the interface feature changes of modified electrodes, because the increase in semicircle diameter of an EIS plot is equal to the increase of the interfacial electron transfer resistance. The Nyquist diagrams of the EIS were obtained in 5 mM $[Fe(CN)_6]^{3-/4-}$ and 1 M KCl at different electrode surfaces. The impedance spectra for all the fabrication steps were investigated by using a Randles equivalent circuit, as displayed in the Figure 1E inset. Therefore, Gamry Echem Analyst software was employed to investigate the EIS results that were fitted with a Randles equivalent circuit. This circuit contains the solution resistance

https://dx.doi.org/10.1021/acsbiomaterials.0c01602
ACS Biomater. Sci. Eng. 2021, 7, 1192−1201

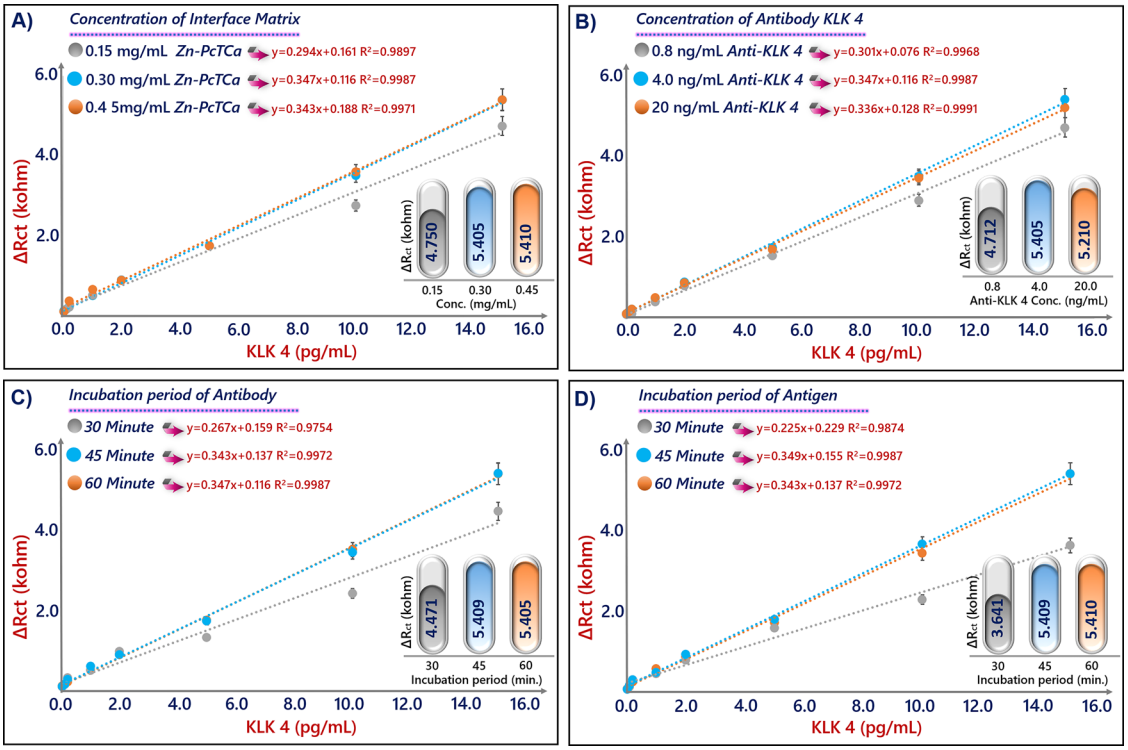

Figure 3. Dependence of immunosensor response on the concentration of Zn-PcTCa (A), anti-KLK (B), incubation duration of anti-KLK (C), and KLK 4 proteins (D).

between working and reference electrodes (R_s), Warburg impedance (W), the constant phase element, and the electron transfer resistance (R_{ct}).[34] The Zn-PcTCa- coated ITO electrode exhibited a small semicircle diameter and illustrated the successful coating of the Zn-PcTCa material. The modification of the electrode surface with Zn-PcTCa provided negatively charged carboxylic groups, and they acted as an electrostatic obstacle that repelled the anions of a redox couple and hindered the ability of the redox couple to access the layer. After activation of carboxyl ends with the NHS/EDC couple, the semicircle diameter further increased due to the charge pushing between the redox couple and negative carboxyl ends. Hence, the electron transfer rate decreased. The immobilization of the anti-KLK 4 protein on the activated ITO electrode induced an increase in semicircle diameter because of the formation of a nonconductive protein layer that acted as an electrostatic barrier and limited the electron transfer between the electrode surface and the redox couple. The application of BSA as a blocker caused an increase in R_{ct} due to its low conductive property. By the attachment of the KLK 4 antigen on the ITO sheet, the R_{ct} value was increased, and this increment indicated the successful formation of an immunocomplex between anti-KLK 4 and KLK 4 proteins.

Apart from EIS, CV measurement was made to follow the electrochemical properties of the modified surfaces. The Zn-PcTCa-modified ITO surface had high peak currents. The peak currents were decreased after the activation of carboxyl groups of Zn-PcTCa. This decrease originated from repulsive interaction between the negatively charged carboxyl ends of Zn-PcTCa and the negatively charged redox couple. Afterward, decreases were seen in the peak currents after adding anti-KLK 4, BSA, and KLK 4 protein molecules, respectively. This phenomenon originated from the hindrance effect of nonconductive biomolecules. The CV results were in accordance with EIS signals, which proved the successful construction of the KLK 4 sensor.

3.3. Morphological Characterization of the Modified Electrodes. SEM and AFM are efficient tools to get the direct visualization information after the modification of electrode surfaces.[13] Figure 2A displays that the spin-coated Zn-PcTCa appeared as a layer, providing a large surface area for the attachment of anti-KLK 4. The average roughness (R_a) of the Zn-PcTCa-modified ITO electrode was 21.9 nm (Figure 2B). The R_a of the bare ITO surface was found as 0.4 nm in our previous work.[35] The R_a value of the Zn-PcTCa-modified ITO electrode was higher than the bare ITO electrode. This increase in the R_a value proved the successful modification of the ITO electrode. After conjugation with anti-KLK 4, the view of the electrode surface was changed, and the anti-KLK 4 antibodies were seen clearly (Figure 2C). The SEM image showed the homogenous layer of the anti-KLK 4 protein onto the ITO surface and antibody structures were aggregated in appearance. The R_a of this step increased because of the aggregated appearance, and it was found as 66.2 nm (Figure 2D). The blockage of carboxyl groups with BSA caused an additional layer on the electrode surface (Figure 2E) and it provided a smooth surface, and therefore, the R_a was measured as 31.2 after BSA immobilization (Figure 2F). After the interaction of the KLK 4 antigen on the ITO/Zn-PcTCa/anti-KLK4/BSA electrode, the view of SEM illustrated a clear layer with KLK 4 antigen molecules (Figure 2G). The specific interaction between the anti-KLK4 antibody and KLK4 antigen increased the R_a value owing to the formed protein layer and it was measured as 130 nm (Figure 2H), and this increment confirmed the successful immobilization of the KLK 4 antigen. Consequently, the change in morphological appearance after each step clearly illustrated the successful modification of all the materials and biomolecules.

https://dx.doi.org/10.1021/acsbiomaterials.0c01602
ACS Biomater. Sci. Eng. 2021, 7, 1192−1201

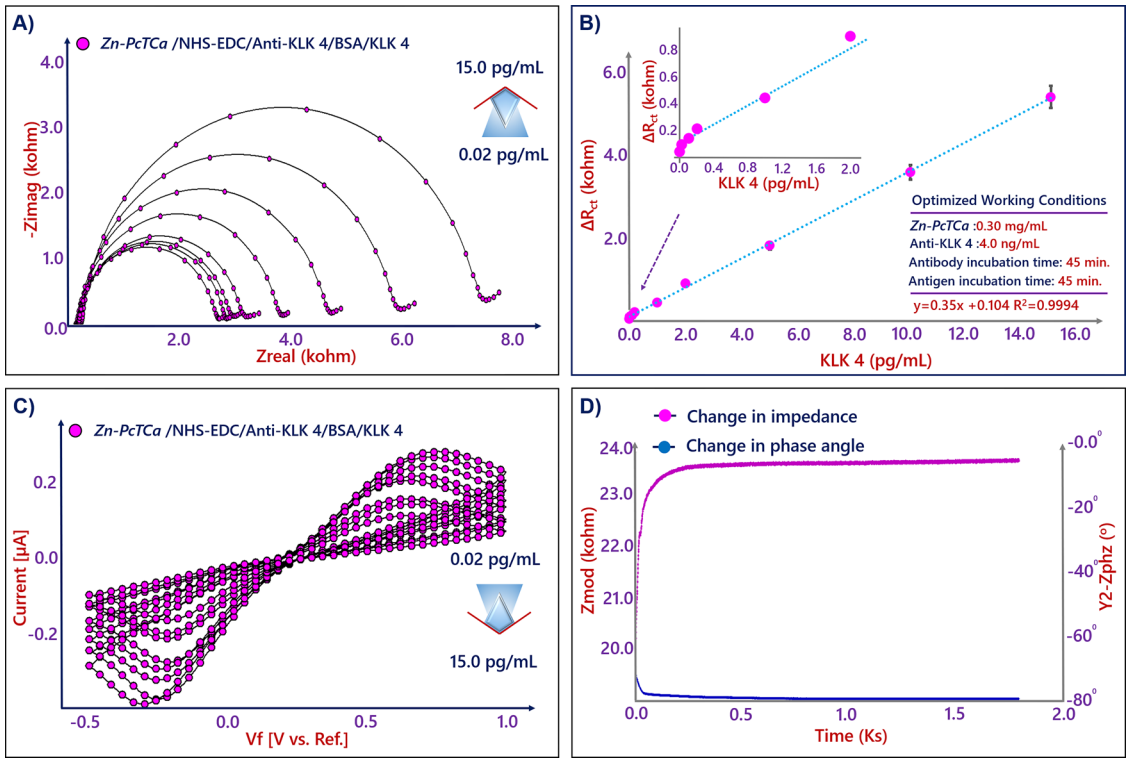

Figure 4. Nyquist plots (A) and CVs (B) of the KLK 4 biosensor for different levels of KLK 4 antigen, the linear relationship between the ΔR_{ct} and the KLK 4 concentration (C), and the SFI analysis result (D).

3.4. Optimization Studies. To reach optimal biosensing performance, some experiments were conducted to determine optimum Zn-PcTCa concentration, the optimal anti-KLK4 amount and the incubation duration, and KLK 4 antigen incubation duration for the interaction with anti-KLK4. First of all, to obtain a maximum impedimetric response, the effect of Zn-PcTCa concentration was investigated, as seen in Figure 3A. In order to obtain a suitable immobilization support, three different Zn-PcTCa amounts (0.15, 0.30, and 0.45 mg/mL) were tried. A low Zn-PcTCa amount caused a low impedimetric response. The increase in Zn-PcTCa concentration caused an increment in the R_{ct} value. The increase of Zn-PcTCa concentration from 0.30 to 0.45 mg/mL did not change the biosensor response. Therefore, 0.30 mg/mL was chosen as the optimum Zn-PcTCa amount for the construction of the KLK 4 immunosensor. Thereafter, the utilized anti-KLK 4 level was optimized. To optimize the amount of anti-KLK 4 loaded on the electrode surface, 0.8, 4, and 20 ng/mL of anti-KLK 4 were used for immunosensor fabrication. As seen in Figure 3B, the R_{ct} increased with the increase in anti-KLK 4 antibody concentration. The responses of 4 ng/mL antibody immobilized electrode and 20 ng/mL antibody immobilized electrode were similar, and therefore 4 ng/mL was selected as the optimum anti-KLK 4 protein concentration. In order to select the optimum anti-KLK 4 antibody incubation time for the biosensor, the biosensor was incubated in phosphate buffer containing 4 ng/mL anti-KLK 4 antibody for different periods of time, and the EIS signal changes were recorded accordingly. The short incubation time (30 min) caused a low signal and the immunosensor response increased with the prolonged time. The responses after 45 min incubation and 60 min incubation were similar, and 45 min incubation in antibody solution offered a high immunosensor signal. Accordingly, 45 min was chosen as the optimum antibody incubation duration (Figure 3C). At last, the incubation duration of KLK 4 antigen was optimized. As shown in Figure 3D, the impedimetric signal of the immunosensor obviously increased when the incubation duration was raised from 30 to 60 min. However, when the time exceeded 45 min, the impedimetric response remained constant. Therefore, 45 min was the optimized time.

3.5. Analytical Studies of the KLK 4 Immunosensor. To analyze the detection limit and linear detection range of the KLK 4 biosensor, the prepared electrodes were incubated with different levels of KLK 4 for 45 min. Figure 4A displays Nyquist plots of the impedance spectra of the ITO/Zn-PcTCa/anti-KLK4/BSA/KLK4 electrode with different concentrations of the KLK 4 antigen. The R_{ct} value raised significantly with higher levels of the KLK 4 antigen because of an increase in coating of the KLK4 antigen−anti-KLK 4 antibody immunocomplex on the ITO electrode surface. Figure 4B illustrated the CVs of the ITO/Zn-PcTCa/anti-KLK4/BSA/KLK4 electrode with different concentrations of the KLK 4 antigen. As seen in Figure 4B, increasing the concentration of the KLK 4 antigen led to decreases in peak currents. The change in the R_{ct} was linear with the KLK 4 antigen level in a range from 0.02 to 15 pg/mL (Figure 4C). The linear regression equation was ΔR_{ct} (kΩ) = 0.351 [KLK 4] (pg/mL) + 0.104, and the regression coefficient was 0.9995. The limit of detection, limit of determination, and sensitivity were found as 6.8 fg/mL (S/N = 3), 22.6 fg/mL (S/N = 10), and 1.44 kΩ pg^{-1} mL cm^{-2}, respectively.

Single frequency impedance (SFI) is employed to determine the variations in electrochemical impedance versus duration. This technique permits the monitoring of online biosensor systems.[24,36] In the present work, a monitor frequency was

https://dx.doi.org/10.1021/acsbiomaterials.0c01602
ACS Biomater. Sci. Eng. 2021, 7, 1192−1201

chosen by using a Bode plot. The increase in impedance (purple) proved the specific immune interaction between the KLK 4 specific antibody and its antigen.

3.6. Repeatability, Reproducibility, Specificity, Stability, and Regeneration of the Immunosensor. To investigate the repeatability of the immunosensor, 20 equally fabricated electrodes illustrated acceptable repeatability in response to the 2 pg/mL KLK 4 biomarker; the relative standard deviation (RSD) was 3.61% (Figure S5A). The reproducibility of the biosensor was examined by preparation of 10 different biosensors and their application to KLK 4 antigens. The RSD was calculated to 1.15% for 10 biosensors (Figure S5B). The result displayed an excellent reproducibility of this biosensor. The specificity of the immunosensor with the KLK 4 antigen and other nonspecific possible antigens, such as IL 6, IL 1α, and PSMA, was carried out as described in EIS measurement. The impedimetric responses of the biosensor after 45 min incubation with 2 pg/mL of the KLK 4 antigen and 200 pg/mL of nonspecific antigens were investigated, and it was found that the proposed immunosensor gave a small signal to the nonspecific antigens (Figure S6).

Stability of the biosensors is an important factor, which affects its performance.[37] For this reason, the stability of the biosensor based on the anti-KLK 4 antibody was studied by measuring the change in the EIS response every week of storage at 4 °C. The immunosensor electrode was found to be stable for 9 weeks at 4 °C only with 21.18% loss in the initial EIS response of the immobilized electrode (Figure S7A). After storage for 9 weeks at 4 °C, there was a decrease in the biosensor response because of activity loss of antibodies. Therefore, morphological change can be observed on the electrode surface.

Regeneration is an important topic in the fields of sensing and biosensing applications.[38] The reusability of an immunosensor eliminates the time-consuming procedure for working electrode preparation and anti-KLK 4 antibody attachment. Multiple regeneration cycles were studied by subjecting the biosensor to KLK 4 antigens and regenerating in HCl solution (10 mM, 5 min) at room temperature. The regeneration process of the suggested immunosensor was studied for six cycles, and 77.94% of the initial signal still remained at the end of the sixth regeneration process. The results showed that the immunosensor could be regenerated for a second use after incubation with acidic solution (Figure S7B). Moreover, we evaluated the morphology of the electrode surfaces before and after the regeneration process. For this purpose, we compared the surface morphologies between before the first measurement of the biosensor (Figure 2E) and after the seventh regeneration process of the same biosensor by using SEM images (Figure S8). We obtained that the morphological appearance of the surface of the biosensor substantially varied after the seventh regeneration process. It is clear that the relatively monolayer of the biosensor surface (Figure 2E) was destroyed after successive regenerations of the surface by using acidic solution.

3.7. Analyses of Serum Samples. To further investigate the reliability of the suggested biosensor, recovery analyses were performed by using the standard addition technique, and the KLK 4 antigen spiked into the 10-fold diluted healthy human serum samples. Each sample was analyzed twice. As shown in Table 1B, the recovery was ranging from 98.14 to 102.88%, indicating that the immunosensor was suitable for determining KLK 4 in real human serum samples.

4. CONCLUSIONS

In summary, we fabricated a simple and sensitive electrochemical biosensor based on an ITO-PET substrate modified with Zn-PcTCa as a new interface matrix for successful immobilization of anti-KLK 4 and the detection of a KLK 4 antigen. Anti-KLK 4 antibodies were covalently immobilized onto this platform due to its carboxyl groups, which were activated by the couple EDC/NHS before the covalent attachment. Under optimum conditions, the suggested method could sensitively detect the KLK 4 antigen from 0.02 to 15 pg/mL with a detection limit of 6.8 fg/mL. The sensitivity of the immunosensor was 1.44 kΩ $pg^{-1}mL\ cm^{-2}$ with EIS and found highly specific to the KLK 4 antigen. Furthermore, the proposed immunosensor was ready to utilize for clinical applications with extremely low cost, easy fabrication procedures, good accuracy, high specificity, and excellent stability Thus, the proposed immunosensor was a promising way for the quantification of KLK 4 in clinical applications.

■ ASSOCIATED CONTENT

Supporting Information

The Supporting Information is available free of charge at https://pubs.acs.org/doi/10.1021/acsbiomaterials.0c01602.

The UV-visible result of the Zn-PcTCa molecule; the FTIR spectrum of the Zn-PcTCa molecule; broad-scan XPS spectra of Zn-PcTCa (a), and graphs (b−e) show the XPS spectra of O 1s, Zn 2p, N 1s, and C 1s; SEM-EDX analysis results of the bare ITO electrode (A) and the Zn-PcTCa interface matrix-coated ITO electrode (B); results of repeatability; specificity of the immunosensor; results of storage stability (A) and regeneration (B); and the morphology of the electrode surface after the seventh regeneration process (PDF)

■ AUTHOR INFORMATION

Corresponding Author

Mustafa Kemal Sezgintürk − *Bioengineering Department, Faculty of Engineering, Çanakkale Onsekiz Mart University, Çanakkale 17100, Turkey;* orcid.org/0000-0003-3042-1087; Email: msezginturk@hotmail.com

Authors

Elif Burcu Aydın − *Scientific and Technological Research Center, Tekirdağ Namık Kemal University, Tekirdağ 59030, Turkey*

Muhammet Aydın − *Scientific and Technological Research Center, Tekirdağ Namık Kemal University, Tekirdağ 59030, Turkey*

Abdulcelil Yuzer − *Department of Natural and Mathematical Sciences, Faculty of Engineering, Tarsus University, Mersin 33400, Turkey*

Mine Ince − *Department of Natural and Mathematical Sciences, Faculty of Engineering, Tarsus University, Mersin 33400, Turkey;* orcid.org/0000-0002-9164-0446

Kasim Ocakoğlu − *Department of Natural and Mathematical Sciences, Faculty of Engineering, Tarsus University, Mersin 33400, Turkey*

Complete contact information is available at: https://pubs.acs.org/10.1021/acsbiomaterials.0c01602

Notes

The authors declare no competing financial interest.

https://dx.doi.org/10.1021/acsbiomaterials.0c01602
ACS Biomater. Sci. Eng. 2021, 7, 1192−1201

■ ACKNOWLEDGMENTS

The authors thank the Scientific and Technological Research Council of Tekirdağ Namık Kemal University, NKU-BAP (NKUBAP.00.ÖNAP.19.209) for the support of this work.

■ REFERENCES

(1) Akbari jonous, Z.; Shayeh, J. S.; Yazdian, F.; Yadegari, A.; Hashemi, M.; Omidi, M. An electrochemical biosensor for prostate cancer biomarker detection using graphene oxide−gold nanostructures. *Eng. Life Sci.* **2019**, *19*, 206−216.

(2) Singh, S.; Gill, A. A. S.; Nlooto, M.; Karpoormath, R. Prostate cancer biomarkers detection using nanoparticles based electrochemical biosensors. *Biosens. Bioelectron.* **2019**, *137*, 213−221.

(3) Razmi, N.; Hasanzadeh, M. Current advancement on diagnosis of ovarian cancer using biosensing of CA 125 biomarker: Analytical approaches. *Trends Anal. Chem.* **2018**, *108*, 1−12.

(4) Nasser, N. J.; Thoms, J.; Soosaipillai, A.; Pintilie, M.; Wang, R.; Diamandis, E. P.; Bristow, R. G. Human tissue Kallikreins: Blood levels and response to radiotherapy in intermediate risk prostate cancer. *Radiotherapy and Oncology* **2017**, *124*, 427−432.

(5) Seiz, L.; Kotzsch, M.; Grebenchtchikov, N. I.; Geurts-Moespot, A. J.; Fuessel, S.; Goettig, P.; Gkazepis, A.; Wirth, M. P.; Schmitt, M.; Lossnitzer, A.; Sweep, F. C. G. J.; Magdolen, V. Polyclonal antibodies against kallikrein-related peptidase 4 (KLK4): immunohistochemical assessment of KLK4 expression in healthy tissues and prostate cancer. *Biol. Chem.* **2010**, *391*, 391−401.

(6) Swedberg, J. E.; Nigon, L. V.; Reid, J. C.; de Veer, S. J.; Walpole, C. M.; Stephens, C. R.; Walsh, T. P.; Takayama, T. K.; Hooper, J. D.; Clements, J. A.; Buckle, A. M.; Harris, J. M. Substrate-guided design of a potent and selective kallikrein-related peptidase inhibitor for kallikrein 4. *Chem. Biol.* **2009**, *16*, 633−643.

(7) Zou, J.; Zhao, G.-Q.; Teng, J.; Liu, Q.; Jiang, X.-Y.; Jiao, F.-P.; Yu, J.-G. Highly sensitive detection of bisphenol A in real water samples based on in-situ assembled graphene nanoplatelets and gold nanoparticles composite. *Microchem. J.* **2019**, *145*, 693−702.

(8) Mounesh; Venugopal Reddy, K. R. The electrochemical investigation of carboxamide-PEG2-biotin-CoPc using composite MWCNTs on modified GCE: the sensitive detections for glucose and hydrogen peroxide. *New J. Chem.* **2020**, *44*, 3330−3340.

(9) Sánchez-Calvo, A.; Costa-García, A.; Blanco-López, M. C. Paper-based electrodes modified with cobalt phthalocyanine colloid for the determination of hydrogen peroxide and glucose. *Analyst* **2020**, *145*, 2716−2724.

(10) Keskin, B.; Okuyucu, O.; Altındal, A.; Erdoğmuş, A. Novel indium (III) phthalocyanines; synthesis, photophysical and humidity sensing properties. *New J. Chem.* **2016**, *40*, 5537−5545.

(11) Li, Y.; Wang, B.; Yu, Z.; Zhou, X.; Kang, D.; Wu, Y.; Chen, Z.; He, C.; Zhou, X. The effects of central metals on ammonia sensing of metallophthalocyanines covalently bonded to graphene oxide hybrids. *RSC Adv.* **2017**, *7*, 34215−34225.

(12) Göktuğ, Ö.; Soganci, T.; Ak, M.; Şener, M. K. Efficient synthesis of EDOT modified ABBB-type unsymmetrical zinc phthalocyanine: optoelectrochromic and glucose sensing properties of its copolymerized film. *New J. Chem.* **2017**, *41*, 14080−14087.

(13) Yang, Y.; Jiang, M.; Cao, K.; Wu, M.; Zhao, C.; Li, H.; Hong, C. An electrochemical immunosensor for CEA detection based on Au-Ag/rGO@ PDA nanocomposites as integrated double signal amplification strategy. *Microchem. J.* **2019**, *151*, 104223.

(14) Niu, Y.; Yang, T.; Ma, S.; Peng, F.; Yi, M.; Wan, M.; Mao, C.; Shen, J. Label-free immunosensor based on hyperbranched polyester for specific detection of α-fetoprotein. *Biosens. Bioelectron.* **2017**, *92*, 1−7.

(15) Kavosi, B.; Hallaj, R.; Teymourian, H.; Salimi, A. Au nanoparticles/PAMAM dendrimer functionalized wired ethylene-amine−viologen as highly efficient interface for ultra-sensitive α-fetoprotein electrochemical immunosensor. *Biosens. Bioelectron.* **2014**, *59*, 389−396.

(16) Karami, P.; Bagheri, H.; Johari-Ahar, M.; Khoshsafar, H.; Arduini, F.; Afkhami, A. Dual-modality impedimetric immunosensor for early detection of prostate-specific antigen and myoglobin markers based on antibody-molecularly imprinted polymer. *Talanta* **2019**, *202*, 111−122.

(17) Han, L.; Wang, D.; Yan, L.; Petrenko, V. A.; Liu, A. Specific phages-based electrochemical impedimetric immunosensors for label-free and ultrasensitive detection of dual prostate-specific antigens. *Sens. Actuators, B Chem* **2019**, *297*, 126727.

(18) Aydın, E. B. Highly sensitive impedimetric immunosensor for determination of interleukin 6 as a cancer biomarker by using conjugated polymer containing epoxy side groups modified disposable ITO electrode. *Talanta* **2020**, 120909.

(19) Yang, T.; Wang, S.; Jin, H.; Bao, W.; Huang, S.; Wang, J. An electrochemical impedance sensor for the label-free ultrasensitive detection of interleukin-6 antigen. *Sens. Actuators, B Chem* **2013**, *178*, 310−315.

(20) Aydın, M.; Aydın, E. B.; Sezgintürk, M. K. A disposable immunosensor using ITO based electrode modified by a star-shaped polymer for analysis of tumor suppressor protein p53 in human serum. *Biosens. Bioelectron.* **2018**, *107*, 1−9.

(21) Cardoso, A. R.; de Sá, M. H.; Sales, M. G. F. An impedimetric molecularly-imprinted biosensor for Interleukin-1β determination, prepared by in-situ electropolymerization on carbon screen-printed electrodes. *Bioelectrochemistry* **2019**, *130*, 107287.

(22) Aydın, M.; Aydın, E. B.; Sezgintürk, M. K. A Highly Selective Poly(thiophene)-graft-Poly(methacrylamide) Polymer Modified ITO Electrode for Neuron Specific Enolase Detection in Human Serum. *Macromol. Biosci.* **2019**, *19*, 1900109.

(23) Aydın, M. A sensitive and selective approach for detection of IL 1α cancer biomarker using disposable ITO electrode modified with epoxy-substituted polythiophene polymer. *Biosens. Bioelectron.* **2019**, *144*, 111675.

(24) Aydın, E. B.; Aydın, M.; Sezgintürk, M. K. Selective and ultrasensitive electrochemical immunosensing of NSE cancer biomarker in human serum using epoxy-substituted poly (pyrrole) polymer modified disposable ITO electrode. *Sens. Actuators, B Chem* **2020**, *306*, 127613.

(25) Valipour, A.; Roushani, M. A glassy carbon immunoelectrode modified with vanadium oxide nanobelts for ultrasensitive voltammetric determination of the core antigen of hepatitis C virus. *Microchim. Acta* **2017**, *184*, 4477−4483.

(26) Valipour, A.; Roushani, M. Using silver nanoparticle and thiol graphene quantum dots nanocomposite as a substratum to load antibody for detection of hepatitis C virus core antigen: electrochemical oxidation of riboflavin was used as redox probe. *Biosens. Bioelectron.* **2017**, *89*, 946−951.

(27) Sarabaegi, M.; Roushani, M.; Hosseini, H.; Hoseini, S. J.; Bahrami, M. Facile synthesis of a covalent organic framework (COF) based on the reaction of melamine and trimesic acid incorporated electrospun nanofiber and its application as an electrochemical tyrosinamide aptasensor. *New J. Chem.* **2020**, *44*, 14922−14927.

(28) Svítková, J.; Ignat, T.; Švorc, L'.; Labuda, J.; Barek, J. Chemical modification of boron-doped diamond electrodes for applications to biosensors and biosensing. *Crit. Rev. Anal. Chem.* **2016**, *46*, 248−256.

(29) Sun, X.; Wang, L.; Tan, Z. Improved synthesis of soluble metal-free/metal phthalocyanine tetracarboxylic acids and their application in the catalytic epoxidation of cyclohexene. *Catal. Lett.* **2015**, *145*, 1094−1102.

(30) Sharman, W. M.; van Lier, J. E. A new procedure for the synthesis of water-soluble tri-cationic and -anionic phthalocyanines. *J. Porphyrins Phthalocyanines* **2012**, *09*, 651−658.

(31) Hosu, I. S.; Wang, Q.; Vasilescu, A.; Peteu, S. F.; Raditoiu, V.; Railian, S.; Zaitsev, V.; Turcheniuk, K.; Wang, Q.; Li, M.; Boukherrouba, R.; Szunerits, S. Cobalt phthalocyanine tetracarboxylic acid modified reduced graphene oxide: a sensitive matrix for the electrocatalytic detection of peroxynitrite and hydrogen peroxide. *RSC Adv.* **2015**, *5*, 1474−1484.

https://dx.doi.org/10.1021/acsbiomaterials.0c01602
ACS Biomater. Sci. Eng. 2021, 7, 1192−1201

(32) Achar, B. N.; Lokesh, K. S. Studies on polymorphic modifications of copper phthalocyanine. *J. Solid State Chem.* **2004**, *177*, 1987−1993.
(33) Klykov, O.; Weller, M. G. Quantification of N-hydroxysuccinimide and N-hydroxysulfosuccinimide by hydrophilic interaction chromatography (HILIC). *Anal. Methods* **2015**, *7*, 6443−6448.
(34) Zhao, F.; Xie, Q.; Xu, M.; Wang, S.; Zhou, J.; Liu, F. RNA aptamer based electrochemical biosensor for sensitive and selective detection of cAMP. *Biosens. Bioelectron.* **2015**, *66*, 238−243.
(35) Aydın, E. B.; Aydın, M.; Sezgintürk, M. K. Fabrication of electrochemical immunosensor based on acid-substituted poly (pyrrole) polymer modified disposable ITO electrode for sensitive detection of CCR4 cancer biomarker in human serum. *Talanta* **2020**, *222*, 121487.
(36) Aydın, M.; Aydın, E. B.; Sezgintürk, M. K. A highly selective electrochemical immunosensor based on conductive carbon black and star PGMA polymer composite material for IL-8 biomarker detection in human serum and saliva. *Biosens. Bioelectron.* **2018**, *117*, 720−728.
(37) Roushani, M.; Valipour, A.; Saedi, Z. Electroanalytical sensing of Cd2+ based on metal−organic framework modified carbon paste electrode. *Sens. Actuators, B Chem* **2016**, *233*, 419−425.
(38) Shahrokhian, S.; Salimian, R. Ultrasensitive detection of cancer biomarkers using conducting polymer/electrochemically reduced graphene oxide-based biosensor: Application toward BRCA1 sensing. *Sens. Actuators, B Chem* **2018**, *266*, 160−169.
(39) Aydın, E. B.; Aydın, M.; Sezgintürk, M. K. Construction of succinimide group substituted polythiophene polymer functionalized sensing platform for ultrasensitive detection of KLK 4 cancer biomarker. *Sens. Actuators, B Chem* **2020**, *325*, 128788.

https://dx.doi.org/10.1021/acsbiomaterials.0c01602
ACS Biomater. Sci. Eng. 2021, 7, 1192−1201